

**Time-resolved photon echoes from donor-bound excitons in ZnO epitaxial layers**S. V. Poltavtsev,<sup>1,2,\*</sup> A. N. Kosarev,<sup>1,3</sup> I. A. Akimov,<sup>1,3</sup> D. R. Yakovlev,<sup>1,3</sup> S. Sadofev,<sup>4</sup> J. Puls,<sup>4</sup>  
S. P. Hoffmann,<sup>5</sup> M. Albert,<sup>5</sup> C. Meier,<sup>5</sup> T. Meier,<sup>5</sup> and M. Bayer<sup>1,3</sup><sup>1</sup>*Experimentelle Physik 2, Technische Universität Dortmund, D-44221 Dortmund, Germany*<sup>2</sup>*Spin Optics Laboratory, St. Petersburg State University, 198504 St. Petersburg, Russia*<sup>3</sup>*Ioffe Physical-Technical Institute, Russian Academy of Sciences, 194021 St. Petersburg, Russia*<sup>4</sup>*AG Photonik, Institut für Physik, Humboldt-Universität zu Berlin, D-12489 Berlin, Germany*<sup>5</sup>*Department Physik & CeOPP, Universität Paderborn, D-33098 Paderborn, Germany*

(Received 12 February 2017; revised manuscript received 29 May 2017; published 21 July 2017)

The coherent optical response from 140 nm and 65 nm thick ZnO epitaxial layers is studied using four-wave-mixing spectroscopy with picosecond temporal resolution. Resonant excitation of neutral donor-bound excitons results in two-pulse and three-pulse photon echoes. For the donor-bound A exciton ( $D^0X_A$ ) at temperature of 1.8 K we evaluate optical coherence times  $T_2 = 33\text{--}50$  ps corresponding to homogeneous line widths of  $13\text{--}19$   $\mu\text{eV}$ , about two orders of magnitude smaller as compared with the inhomogeneous broadening of the optical transitions. The coherent dynamics is determined mainly by the population decay with time  $T_1 = 30\text{--}40$  ps, while pure dephasing is negligible. Temperature increase leads to a significant shortening of  $T_2$  due to interaction with acoustic phonons. In contrast, the loss of coherence of the donor-bound B exciton ( $D^0X_B$ ) is significantly faster ( $T_2 = 3.6$  ps) and governed by pure dephasing processes.

DOI: [10.1103/PhysRevB.96.035203](https://doi.org/10.1103/PhysRevB.96.035203)**I. INTRODUCTION**

The optical properties of ZnO are of great interest for applications in ultraviolet (UV) light emitting devices [1,2], polariton lasers [3], UV-sensitive photodetectors [4], and other photonic devices [5]. The main feature of this material is the large exciton binding energy of  $\sim 60$  meV [6], so that exciton emission occurs even at room temperature [7,8]. Another remarkable property is the large exciton oscillator strength resulting in short optical lifetimes, which could be useful in applications requiring fast coherent control.

So far, the coherent optical properties of ZnO were studied on free excitons with short coherence times up to few ps [9–12]. Optical excitation with spectrally broad femtosecond pulses was implemented and, consequently, quantum beats between various exciton states as well as strong many-body interactions were demonstrated [10,11]. For exciton complexes bound to impurities, e.g., donor-bound excitons, long-lived coherence is expected [13]. In order to study distinct states exhibiting long coherence times, four-wave-mixing (FWM) spectroscopy is preferentially performed with resonant excitation of the exciton complex of interest using spectrally narrow pulses, even though the time resolution is reduced thereby. Furthermore, to overcome the large inhomogeneity of exciton transitions, which represents another intrinsic property of ZnO leading to sub-ps decay of macroscopic polarization, photon echo-based techniques are the best choice for studying the coherent dynamics of excitons [14].

In this paper, we demonstrate that for resonant optical excitation of the donor-bound A and B excitons in ZnO epitaxial layers with ps pulses the coherent response is given by photon echoes. The decay of the photon echo signals allows one to determine intrinsic properties of the single donor-bound excitons, such as the coherence time  $T_2$  and population decay

time  $T_1$ . At temperature of 1.8 K, the coherence time of the A bound exciton ( $D^0X_A$ ) is in the range of several tens of ps, corresponding to a homogeneous linewidth of about  $10\text{--}20$   $\mu\text{eV}$ , which is two orders of magnitude smaller than the inhomogeneous broadening of  $D^0X_A$ . Our findings demonstrate that the  $D^0X_A$  in ZnO represents a promising two-level system, which may be used for ultrafast optical control. In contrast, the decoherence of  $D^0X_B$  occurs one order of magnitude faster, while the population decay is approximately the same. In addition, we show that a temperature increase leads to significant shortening of the coherence times due to interactions with phonons.

**II. SAMPLES AND METHOD**

For our study of localized exciton states in bulk ZnO, we used two O-polar ZnO epilayers grown by plasma-assisted molecular-beam epitaxy on *c*-plane (0001) sapphire substrates. Sample I fabricated in Berlin (ZMO1031) is a 140 nm thick ZnO epitaxial layer surrounded by  $\text{Zn}_{0.9}\text{Mg}_{0.1}\text{O}$  layers with thicknesses of 100 nm and  $1$   $\mu\text{m}$  from top and bottom, respectively. Sample II fabricated in Paderborn (ZnO-385) is a 65 nm thick ZnO layer separated from the substrate by a 45 nm thick buffer of low-temperature grown ZnO. Both samples are deposited with a 1–2 nm thick MgO nucleation layer. High-resolution x-ray diffractometry (HR-XRD) demonstrates a high structural quality of both samples (the rocking curves display line widths of 190 arcsec for both samples). Details of this analysis can be found in the Appendix.

The coherent optical response was measured using a three-pulse degenerate FWM setup in reflection geometry. The samples were inserted in a helium bath cryostat and cooled down to 1.8 K. As laser source we used a Ti:Sapphire laser Mira-900 with pulse repetition rate of 75.75 MHz combined with an external second-harmonic generation unit, which delivered frequency-doubled pulses in ultraviolet spectral range with 1.3 ps duration. Optical excitation of the samples was done

\*sergei.poltavtcev@tu-dortmund.de

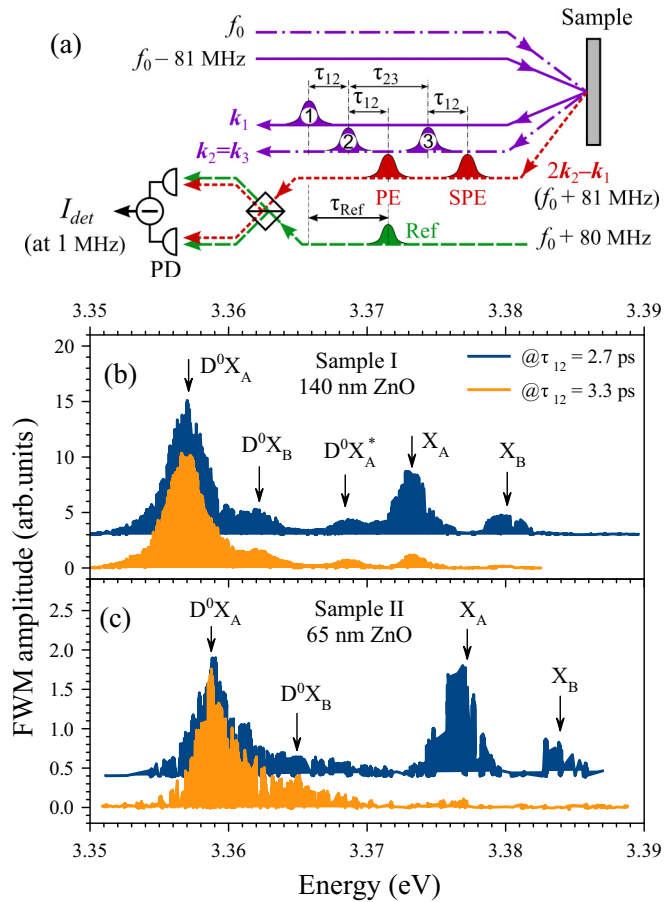


FIG. 1. Time-resolved FWM spectroscopy in ZnO: (a) Schematic of heterodyne time-resolved FWM experiment.  $f_0$  is optical frequency of laser pulse. PD denotes photodetector. (b) and (c) FWM spectra of samples I and II, respectively, measured at second pulse delays  $\tau_{12} = 2.7$  ps and 3.3 ps. FWM detection was performed at  $2\tau_{12}$ . Arrows indicate transitions for  $X_A$ ,  $X_B$ ,  $D^0X_A$ ,  $D^0X_B$ , and  $D^0X_A^*$ .  $T = 1.8$  K.

either by two pulses separated by time  $\tau_{12}$  in the two-pulse photon echo (PE) experiment or by three pulses (the second and third pulses separated by  $\tau_{23}$ ) in the stimulated photon echo (SPE) experiment [15], as schematically shown in Fig. 1(a). The laser photon energy was tuned in the spectral range of the free and donor-bound excitons in ZnO: 3.35–3.39 eV. The first ( $k_1$ ) and second ( $k_2$ ) pulses hit the sample under angles of  $\sim 3^\circ$  and  $4^\circ$ , respectively, in a spot of about  $250 \mu\text{m}$  diameter. The third pulse was collinear with the second one,  $k_3 = k_2$ . The FWM signal was detected along the  $k_{\text{FWM}} = 2k_2 - k_1$  direction. The energy of the exciting pulses was kept below 26 pJ per pulse corresponding to the linear excitation regime for each pulse ( $\chi^{(3)}$  regime). To detect the weak FWM signal, optical heterodyning and interference with a reference laser pulse were exploited [16,17]. Optical heterodyning was accomplished with two acousto-optical modulators (AOMs) acting as optical frequency shifters. The optical frequency of the first pulse was shifted to  $f_1 = f_0 - 81$  MHz with the first AOM, while the optical frequency of the reference pulse separated by  $\tau_{\text{Ref}}$  from the first pulse was shifted to  $f_{\text{Ref}} = f_0 + 80$  MHz with the second AOM. Thus, the optical

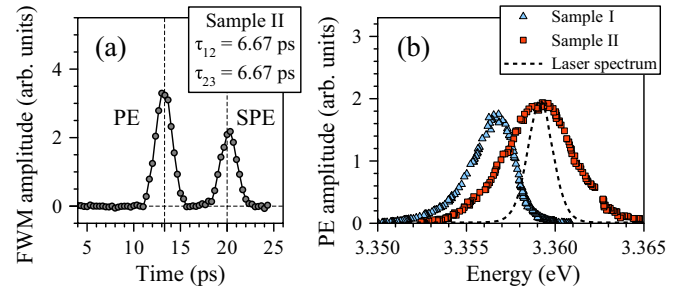


FIG. 2. Photon echo measurements on  $D^0X_A$ : (a) FWM transient measured in three-pulse configuration on sample II at  $\tau_{12} = \tau_{23} = 6.67$  ps. (b) PE spectra measured at  $\tau_{12} = 26.7$  ps and  $\tau_{12} = 13.3$  ps for samples I and II, respectively. Spectrum of ps pulses is shown with dashed line.

frequency of the FWM signal is given by  $f_{\text{FWM}} = 2f_0 - f_1 = f_0 + 81$  MHz. The FWM and the reference beams were mixed in a silicon photodetector and the modulus of the cross correlation of the FWM optical field with the reference pulse field,  $I_{\text{det}}$ , was detected at 1 MHz frequency by a fast lock-in amplifier. Additionally, the first beam was modulated by an optical chopper at 1 kHz frequency, at which synchronous detection by a slow lock-in amplifier was done. All beams were linearly copolarized.

### III. EXPERIMENTAL RESULTS

Figures 1(b) and 1(c) show FWM spectra measured at  $\tau_{\text{Ref}} = 2\tau_{12}$  on both samples for short  $\tau_{12}$  delays of 2.7 ps and 3.3 ps. Four main transitions are seen in the spectra associated with the free A exciton ( $X_A$ ), free B exciton ( $X_B$ ), neutral donor-bound A exciton ( $D^0X_A$ ), and neutral donor-bound B exciton ( $D^0X_B$ ), in good correspondence with the absorption spectrum measured on sample I [18]. Additional transition is seen for sample I at  $\sim 3.369$  eV (about 11.7 meV above  $D^0X_A$ ), as previously observed in photoluminescence excitation spectra and attributed to an excited  $d$  state of the donor-bound exciton A ( $D^0X_A^*$ ) [18–20]. Wagner *et al.* give the values for the zero-stress energies of excitons A and B in ZnO equal to 3.375 eV and 3.382 eV, respectively, measured at  $T = 4$  K [21]. Corresponding exciton resonances in 140 nm ZnO layer (sample I) display about 2 meV red shift, while those in 65 nm layer (sample II) display about 2 meV blue shift, which we attribute to the presence of residual strain in the samples. The free A and B exciton signals decay extremely fast on sub-ps timescale, so that they are already significantly damped in FWM when measured at  $\tau_{12} = 3.3$  ps. We estimate the coherence times of these free excitons to be below 1 ps, in line with previous studies [9–11]. Donor-bound excitons decay significantly slower so that they can be studied in detail with our time-resolved photon echo technique.

The FWM signal from  $D^0X_A$  in form of photon echoes was observed on both samples. Figure 2(a) displays the FWM amplitude transient measured on sample II in the three-pulse echo experiment at  $\tau_{12} = \tau_{23} = 6.67$  ps. This transient is composed of two echo pulses located at the times of the PE ( $2\tau_{12} = 13.3$  ps) and the SPE ( $2\tau_{12} + \tau_{23} = 20$  ps). The temporal profiles of PE and SPE are well fitted with Gaussians with a full width at half maximum (FWHM) of 2.1 ps. In this

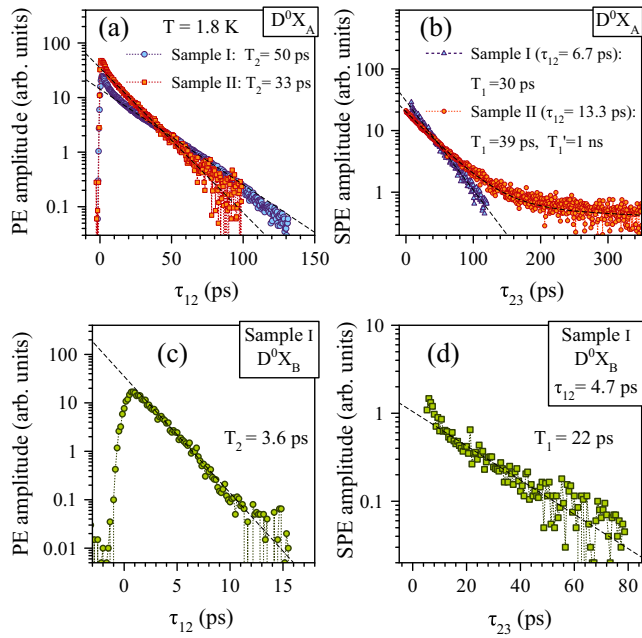


FIG. 3. PE and SPE amplitude decays measured at  $T = 1.8$  K as function of delays  $\tau_{12}$  and  $\tau_{23}$ , respectively. (a) PE decays and (b) SPE decays measured for  $D^0X_A$  in samples I and II. (c) PE decay and (d) SPE decay measured from  $D^0X_B$  (3.3627 eV) in sample I.  $\tau_{12}$  delays used and decay times extracted from exponential fits are given in panels.

case the excited ensemble is defined by the laser spectrum, i.e., the latter is narrower than the inhomogeneous width of the optical transitions. Figure 2(b) shows PE spectra measured at  $\tau_{12} = 26.7$  ps for sample I and 13.3 ps for sample II. The spectral resolution in these measurements is given by the 1.7 meV FWHM of the laser spectrum, shown by the dashed line. Accordingly, in sample I the inhomogeneous broadening of optical transitions is smaller, which we attribute to weaker strain gradients across the ZnO epilayer due to presence of the intermediate ZnMgO buffer layer.

To measure the  $T_2$  and  $T_1$  times of the donor-bound excitons, we either vary the  $\tau_{12}$  delay with PE amplitude detection or the  $\tau_{23}$  delay with SPE amplitude detection. These data are summarized in Fig. 3.  $D^0X_A$  PE decays measured on both samples in the two-pulse echo experiment are shown in Fig. 3(a). Both curves can be well described by monoexponential decays, from which coherence times of  $T_2 = 50 \pm 0.5$  ps for sample I and  $33 \pm 0.5$  ps for sample II can be extracted. These correspond to homogeneous line widths  $\gamma_{D^0X_A} = \hbar/T_2 = 13\text{--}19 \mu\text{eV}$ , respectively. We emphasize that these values are about two orders of magnitude smaller than the inhomogeneous widths of the optical transitions ( $\sim 1$  meV). The small difference in decoherence rates in the two samples can originate from different levels of impurities and defects. Although HR-XRD detects a comparable overall crystal quality of the both samples, the concentration of impurities may differ since the structures were grown under different conditions and have different design.

Figure 3(b) demonstrates the SPE decays measured at  $\tau_{12} = 6.67$  ps and 13.3 ps for samples I and II, respectively. The extracted decay times are  $T_1 = 30 \pm 0.5$  ps for sample I and

$T_1 = 39 \pm 1$  ps for sample II. Sample II exhibits additionally a long-lived component with small amplitude decaying on a  $1000 \pm 200$  ps timescale, which can be explained as follows: The first and second laser pulses create a spectral exciton population grating. During exciton decay, nonradiative relaxation processes can partially empty the excited state, leaving the ground state uncompensated even after exciton recombination [22,23]. The uncompensated spectral grating in the ground state can contribute to the long-lived echo component. This observation additionally hints at a larger concentration of defects, e.g., deep impurities, in sample II.

For the  $D^0X_A$  transition in sample I  $T_2 \approx 2T_1$  and, therefore, we conclude that pure dephasing processes, i.e., elastic scattering of excitons, can be neglected. Thus, the loss of coherence is attributed to the exciton population dynamics, namely energy relaxation including also radiative decay. Interestingly, the value of  $T_1 = 30$  ps is about 4–5 times shorter than the lifetime  $\tau_0 \approx 140$  ps measured by time-resolved photoluminescence using a streak camera on the same sample [18] and the  $\tau_0 \approx 160$  ps for a similar ZnO epilayer [19]. This difference indicates that the SPE decay time  $T_1$  observed here is limited not only by the exciton lifetime, but also by other energy relaxation processes, to which the photoluminescence is insensitive. The relaxation mechanisms behind this exciton decay shortening require further studies.

Next, we compare the coherence of  $D^0X_A$  and  $D^0X_B$  in sample I. Figures 3(c) and 3(d) show the PE and SPE decays at the  $D^0X_B$  optical transition, respectively. From exponential fits we evaluate a coherence time of  $T_2 \approx 3.6$  ps and a population decay time  $T_1 \approx 22$  ps for  $D^0X_B$ . Thus, the homogeneous linewidth of the optical transition,  $\gamma_{D^0X_B} = 180 \mu\text{eV}$ , is about an order of magnitude larger than  $\gamma_{D^0X_A}$ . The fast decoherence of  $D^0X_B$  cannot be attributed to energy relaxation because the population decay remains approximately the same as for  $D^0X_A$ . Therefore, in contrast to  $D^0X_A$ , pure dephasing dominates for  $D^0X_B$ . This is a surprising result because the A and B donor-bound excitons have similar binding energies and, therefore, occupy the same localization volume. A possible explanation for this unexpected behavior is that the  $D^0X_B$  states are located in close proximity to  $D^0X_A$  excited states [20]. Coupling of these states could explain the faster loss of coherence of  $D^0X_B$ .

Finally, to get deeper insight into the coherence properties of donor-bound excitons, we study the PE decay rate in sample I as a function of temperature and optical excitation intensity. The temperature dependences of coherence and population decay times measured on  $D^0X_A$  are shown in Fig. 4(a). While  $T_1$  is temperature independent up to 12 K, the coherence time decreases as  $\sim 1/T$  in accord with the linear increase of the acoustic phonon population leading to pure dephasing of the excitons. As already mentioned before, at  $T = 1.8$  K,  $T_2 \approx 2T_1$  indicating that additional irreversible dephasing mechanisms are negligible. Additionally, we have verified that both times,  $T_2$  and  $T_1$ , are independent of optical excitation intensity as demonstrated in Fig. 4(b) for variation of the first pulse intensity over almost one order of magnitude. We also checked that these times remain the same even when the second and third pulse powers are increased up to several tens of pJ. Thereby, we validate the simple analysis of  $T_2$  and  $T_1$  used in our study. For the localized and disordered systems

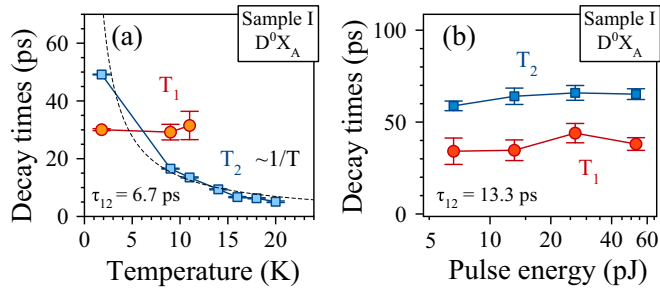


FIG. 4. Results of PE and SPE decay measurements at  $D^0X_A$  transition in sample I. (a) Temperature dependence of  $T_1$  and  $T_2$  times. Dashed line is fit to  $T_2(T)$  data with  $\sim 1/T$ . (b) Dependence of  $T_1$  and  $T_2$  on the first pulse energy. Energies of second and third pulses are below 8 pJ.

investigated here and the chosen excitation conditions it is not expected that many-body phenomena, which would require a much more complex theoretical analysis, will significantly influence the measured signals.

#### IV. CONCLUSIONS

Epitaxial ZnO layers were studied using coherent optical spectroscopy. Two-pulse and three-pulse photon echoes were observed from the donor-bound A and B excitons.  $D^0X_A$  shows a coherent dynamics on time scales of several tens of picoseconds, corresponding to a homogeneous linewidth of 13–19  $\mu\text{eV}$  at  $T = 1.8$  K. On the contrary, the  $D^0X_B$  dephasing is much faster than that for  $D^0X_A$  ( $T_2 = 3.6$  ps and 50 ps, respectively), whereas the population decay times are comparable ( $T_1 = 33$  ps for  $D^0X_A$  and 22 ps for  $D^0X_B$ ). This indicates that pure dephasing dominates for  $D^0X_B$ , in contrast to  $D^0X_A$ . We also show that acoustic phonons play important role, limiting the donor-bound exciton coherence in ZnO at elevated temperatures. In comparison with other wide-band-gap wurtzite semiconductors, CdS was reported to show a coherence time of 800 ps, comparable with its lifetime of 1000 ps, for the neutral acceptor-bound exciton [24]. Due to the much larger oscillator strength, the coherent optical dynamics of the donor-bound exciton in ZnO is significantly shorter lived, making ZnO an attractive candidate for fast coherent control as compared to other wide-band-gap semiconductors.

#### ACKNOWLEDGMENTS

We are grateful to A. V. Rodina for useful discussions. We acknowledge the financial support of the Deutsche Forschungsgemeinschaft (DFG) through the Collaborative Research Centre TRR 142 (Project A02). S.V.P. thanks the

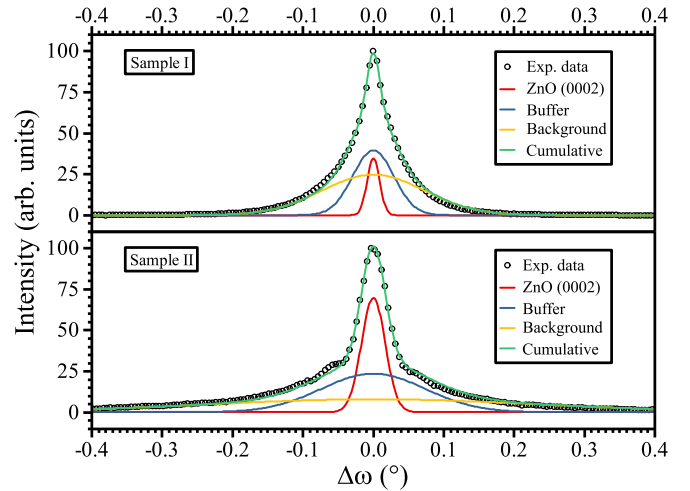


FIG. 5.  $\omega$  scans (rocking curves) of the (0002) reflection measured on both samples by HR-XRD method. Dots correspond to the experimental data; fitting curve (green line) is a sum of three contributions: signal from ZnO layer (red line), buffer layer (blue line), and a background (orange line).

Russian Foundation of Basic Research for partial financial support (Contract No. 15-52-12016 NNIO\_a). M.B. acknowledges the partial financial support from the Russian Ministry of Science and Education (Contract No. 14.Z50.31.0021). J.P. and S.S. thank the DFG in the frame of SFB 951 (HIOS) for the funding.

#### APPENDIX: STRUCTURAL X-RAY ANALYSIS

The structural analysis performed by HR-XRD reveals a high overall crystalline perfection for both samples. Figure 5 shows  $\omega$  scans (rocking curves) of the (0002) reflection. The spectra exhibit strongly non-Gaussian line shape typical for ZnO epitaxial layers grown on  $c$ -plane sapphire with a MgO nucleation layer, where most relaxation processes occur at the interface with sapphire [25]. The large background signal (sample I) originates from a contribution of the ZnMgO buffer layer, which cannot be completely eliminated due to the small separation between the ZnO and ZnMgO (0002) reflections. The FWHMs extracted from the  $\omega$  scans are 190 arcsec for both samples indicating practically an identical crystal quality. A strain analysis was done based on comparison of the lattice constants obtained from  $\omega - 2\theta$ -scan measurements with the unstrained value  $c_0 \approx 5.204$  Å given in the literature [26]. Values of  $c$ -lattice constant measured for samples I and II are 5.2053 Å and 5.2006 Å, respectively, indicating the presence of a larger strain in sample II. The lower strain in sample I can be explained by the presence of the significantly thicker buffer layer.

[1] A. Tsukazaki, A. Ohtomo, T. Onuma, M. Ohtani, T. Makino, M. Sumiya, K. Ohtani, S. F. Chichibu, S. Fuke, Y. Segawa, H. Ohno, H. Koinuma, and M. Kawasaki, Repeated temperature modulation epitaxy for p-type doping and

light-emitting diode based on ZnO, *Nature Mater.* **4**, 42 (2005).

[2] Y. Ryu, T.-S. Lee, J. A. Lubguban, H. W. White, B.-J. Kim, Y.-S. Park, and C.-J. Youn, Next generation of oxide photonic devices:

- ZnO-based ultraviolet light emitting diodes, *Appl. Phys. Lett.* **88**, 241108 (2006).
- [3] P. Bhattacharya, T. Frost, S. Deshpande, M. Z. Baten, A. Hazari, and A. Das, Room Temperature Electrically Injected Polariton Laser, *Phys. Rev. Lett.* **112**, 236802 (2014).
- [4] P. Sharma, A. Mansingh, and K. Sreenivas, Ultraviolet photoresponse of porous ZnO thin films prepared by unbalanced magnetron sputtering, *Appl. Phys. Lett.* **80**, 553 (2002).
- [5] C. Klingshirn, ZnO: From basics towards applications, *Phys. Status Solidi B* **244**, 3027 (2007).
- [6] D. Thomas, The exciton spectrum of zinc oxide, *J. Phys. Chem. Solids* **15**, 86 (1960).
- [7] B. K. Meyer, H. Alves, D. M. Hofmann, W. Kriegseis, D. Forster, F. Bertram, J. Christen, A. Hoffmann, M. Straburg, M. Dworzak, U. Haboek, and A. V. Rodina, Bound exciton and donor-acceptor pair recombinations in ZnO, *Phys. Status Solidi B* **241**, 231 (2004).
- [8] J. Cui, S. Sadofev, S. Blumstengel, J. Puls, and F. Henneberger, Optical gain and lasing of ZnO/ZnMgO multiple quantum wells: From low to room temperature, *Appl. Phys. Lett.* **89**, 051108 (2006).
- [9] W. Zhang, H. Wang, K. S. Wong, Z. K. Tang, G. K. L. Wong, and R. Jain, Third-order optical nonlinearity in ZnO microcrystallite thin films, *Appl. Phys. Lett.* **75**, 3321 (1999).
- [10] K. Hazu, T. Sota, S. Adachi, S. Chichibu, G. Cantwell, D. C. Reynolds, and C. W. Litton, Phonon scattering of excitons and biexcitons in ZnO, *J. Appl. Phys.* **96**, 1270 (2004).
- [11] E. Mallet, P. Disseix, D. Lagarde, M. Mihailovic, F. Réveret, T. V. Shubina, and J. Leymarie, Accurate determination of homogeneous and inhomogeneous excitonic broadening in ZnO by linear and nonlinear spectroscopies, *Phys. Rev. B* **87**, 161202 (2013).
- [12] I. Popov, N. Vashurin, S. Putilin, S. Stepanov, V. Sidorova, and N. Sushentsov, Photon echoes in single- and trilayer semiconductor films of different nanosized thicknesses and their properties, *Bull. Rus. Acad. Sci.: Phys.* **78**, 152 (2014).
- [13] G. Noll, U. Siegner, S. G. Shevel, and E. O. Göbel, Picosecond Stimulated Photon Echo Due to Intrinsic Excitations in Semiconductor Mixed Crystals, *Phys. Rev. Lett.* **64**, 792 (1990).
- [14] M. Koch, D. Weber, J. Feldmann, E. O. Göbel, T. Meier, A. Schulze, P. Thomas, S. Schmitt-Rink, and K. Ploog, Subpicosecond photon-echo spectroscopy on GaAs/AlAs short-period superlattices, *Phys. Rev. B* **47**, 1532 (1993).
- [15] P. R. Berman and V. S. Malinovsky, *Principles of Laser Spectroscopy and Quantum Optics* (Princeton University Press, Princeton, 2011).
- [16] M. Hofmann, S. D. Brorson, J. Mørk, and A. Mecozzi, Time resolved four-wave mixing technique to measure the ultrafast coherent dynamics in semiconductor optical amplifiers, *Appl. Phys. Lett.* **68**, 3236 (1996).
- [17] L. Langer, S. V. Poltavtsev, I. A. Yugova, D. R. Yakovlev, G. Karczewski, T. Wojtowicz, J. Kossut, I. A. Akimov, and M. Bayer, Magnetic-Field Control of Photon Echo From the Electron-Trion System in a CdTe Quantum Well: Shuffling Coherence Between Optically Accessible and Inaccessible States, *Phys. Rev. Lett.* **109**, 157403 (2012).
- [18] J. Kim, J. Puls, S. Sadofev, and F. Henneberger, Charged carrier spin dynamics in ZnO quantum wells and epilayers, *Phys. Rev. B* **93**, 045306 (2016).
- [19] D. Lagarde, A. Balocchi, P. Renucci, H. Carrère, F. Zhao, T. Amand, X. Marie, Z. X. Mei, X. L. Du, and Q. K. Xue, Exciton and hole spin dynamics in ZnO investigated by time-resolved photoluminescence experiments, *Phys. Rev. B* **78**, 033203 (2008).
- [20] B. K. Meyer, J. Sann, S. Eisermann, S. Lautenschlaeger, M. R. Wagner, M. Kaiser, G. Callsen, J. S. Reparaz, and A. Hoffmann, Excited state properties of donor bound excitons in ZnO, *Phys. Rev. B* **82**, 115207 (2010).
- [21] M. R. Wagner, G. Callsen, J. S. Reparaz, R. Kirste, A. Hoffmann, A. V. Rodina, A. Schleife, F. Bechstedt, and M. R. Phillips, Effects of strain on the valence band structure and exciton-polariton energies in ZnO, *Phys. Rev. B* **88**, 235210 (2013).
- [22] J. Morsink, W. Hesselink, and D. Wiersma, Photon echo stimulated from optically induced nuclear spin polarization, *Chem. Phys. Lett.* **64**, 1 (1979).
- [23] L. Langer, S. V. Poltavtsev, I. A. Yugova, M. Salewski, D. R. Yakovlev, G. Karczewski, T. Wojtowicz, I. A. Akimov, and M. Bayer, Access to long-term optical memories using photon echoes retrieved from semiconductor spins, *Nature Photon.* **8**, 851 (2014).
- [24] A. Hoffmann, V. Kutzer, and A. Göldner, Excitons in wide-gap II-VI and nitride semiconductors. Comparison of optical studies of shallow dopants in these materials, *Phys. Status Solidi B* **210**, 327 (1998).
- [25] Y. Chen, H.-J. Ko, S.-K. Hong, and T. Yao, Layer-by-layer growth of ZnO epilayer on Al<sub>2</sub>O<sub>3</sub>(0001) by using a MgO buffer layer, *Appl. Phys. Lett.* **76**, 559 (2000).
- [26] H. Karzel, W. Potzel, M. Köfferlein, W. Schiessl, M. Steiner, U. Hiller, and G. M. Kalvius, D. W. Mitchell, T. P. Das, P. Blaha, K. Schwarz, and M. P. Pasternak, Lattice dynamics and hyperfine interactions in ZnO and ZnSe at high external pressures, *Phys. Rev. B* **53**, 11425 (1996).